Advances in Nuclear Fuel Management III (ANFM 2003)
Hilton Head Island, South Carolina, USA, October 5-8, 2003, on CD-ROM, American Nuclear Society, LaGrange Park, IL (2003)

Equilibrium Cycle Analysis with XIMAGE/SIMAN

John G. Stevens and Ken R. Rempe
Studsvik Scandpower, Inc.
504 Shoup Avenue, Suite 201
Idaho Falls, Idaho 83402
john@soa.com ken@soa.com

Keywords: Loading Pattern Design, Equilibrium Analysis, Optimization

ABSTRACT

Commercial LWR core design tools [1-3] continue to evolve due to demands for increased cycle performance even as operational experience has introduced new limiting design constraints related to:: fuel bowing; vessel fluence; PWR fuel steaming; or cross-quadrant shuffling requirements/restrictions to mitigate core tilts. A key ongoing concern is that improved single cycle designs should not adversely affect multicycle and equilibrium performance.

This paper briefly reviews the capabilities of the XIMAGE/SIMAN core design code, with emphasis on recent enhancements related to emerging design constraints. Automation of equilibrium cycle energy analysis is then discussed. Finally, examples of the equilibrium energy performance for cores at different levels of optimization are presented.

1. SINGLE CYCLE DESIGN FOR BWR AND PWR CORES WITH XIMAGE

XIMAGE [2,4] provides the unique combination of 1) a graphical interface with direct linkage to advanced nodal analysis including feedbacks and pin reconstruction; 2) multicycle framework allowing detailed design of individual loading patterns within a sequence of scoping cycles; and 3) a highly configurable autoloader to generate patterns which satisfy a target k_∞ distribution subject to a loading strategy of user-specified rules and heuristics.

Because XIMAGE uses the SIMULATE-3 [Ref. 5] advanced nodal code directly with CASMO-4 [Ref. 6] cross sections, a large set of design parameters may be tracked accurately during design. For BWRs, thermal limits and shutdown margins are of greatest interest. For PWRs pin peaking factors, power dependent peaking limits and steaming rates often limit designs.

Figure 1 illustrates the main window for an XIMAGE BWR session. The interface has been enhanced to facilitate design of large cores, such as BWR half-cores. Data filtering allows significant data to be viewed more readily, by suppressing “insignificant” data. Envelope tracking (i.e., display of worst ratio to a limit throughout depletion) and simple scrolling through depletions facilitate difficult reactivity control design.

XIMAGE continues to evolve as new design constraints become limiting. For instance, the peripheral history of each face of each assembly is now tracked, and optional rules can preclude repeated use of the same face on the periphery (to avoid bowing) or placement of faces which would “sandwich” a BWR control blade or detector between two faces prone to bowing.

Table 1 lists the key rules available to direct the XIMAGE Autoloader. Compliance to rules is tracked for all patterns evaluated in XIMAGE, so a rule set is valuable as a tool to monitor adherence to a strategy or design checklist. Custom rule modules have also been implemented to track metrics which can help avoid quadrant power tilts.

A key emerging concern for many PWRs is crud deposition associated with subcooled boiling. The crud can exacerbate corrosion and may contribute to axial offset anomalies. An optional steaming rate model[7] has been added to SIMULATE-3 and XIMAGE PWR to calculate and display the rate of subcooled boiling. Steaming rates can be tracked within regions of assemblies so that peak face rates can be displayed, for instance.

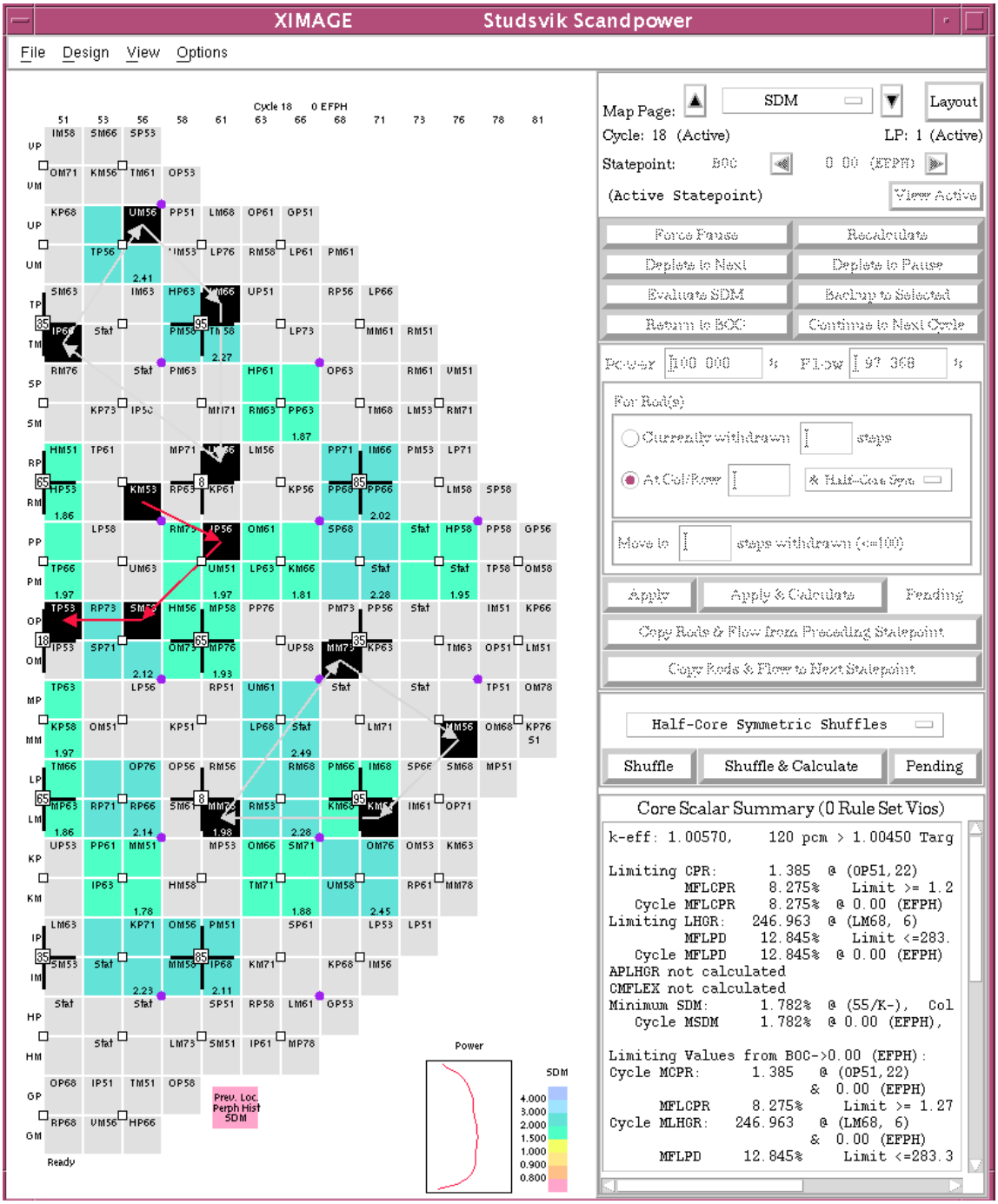

Fig. 1: Main Interface Window of an XIMAGE BWR Session

Table 1: Key Rule Set Components for the Autoloader and/or LP Verification

Description	BWR	PWR
Require stationary bundles, i.e., no shuffle (n-1)->n Important for min. shuffle design or fluence control.	Y	Y
Exclusion of peripheral history, either face specific or general exclusion. Important due to bowing.	Y	Y
Exclusion of bundles which have been used in a control cell. For axial shape and bow concerns.	Y	
Fix/Exclude a batch in/from a position. Used mainly to enforce strategy, but also useful for lead test assemblies or similar restrictions.	Y	Y
Symmetry requirements by batch, fuel type, and/or properties.	Y	Y
Fix/Exclude orientation of assembly quadrant with minimum exposure (e.g., demand cold periphery).		Y
Max. exposure or k_∞ allowed in a position. Used for strategy or to avoid problems in rodded positions.	Y	Y
Relational heuristics preclude combinations, such as face-adjacent pairs or a mix-of-four in a control cell.	Y	Y
Position lock to facilitate design progress.	Y	Y

2. AUTOMATED EQUILIBRIUM ANALYSIS WITH XIMAGE

XIMAGE has always been a multicycle tool. Techniques for the development of transition and equilibrium cycles were described in Reference 4. But there were two key limitations to the equilibrium capabilities. First, the user had to create at least a minimal rule set and a variety of cycle specific input in order to invoke a multicycle analysis. Second, and more significant, changes to strategy at the equilibrium state were not automatically applied during a redepletion from the start of scoping through equilibrium.

Figure 2 illustrates the automated equilibrium process recently added to XIMAGE for BWR and PWR application.

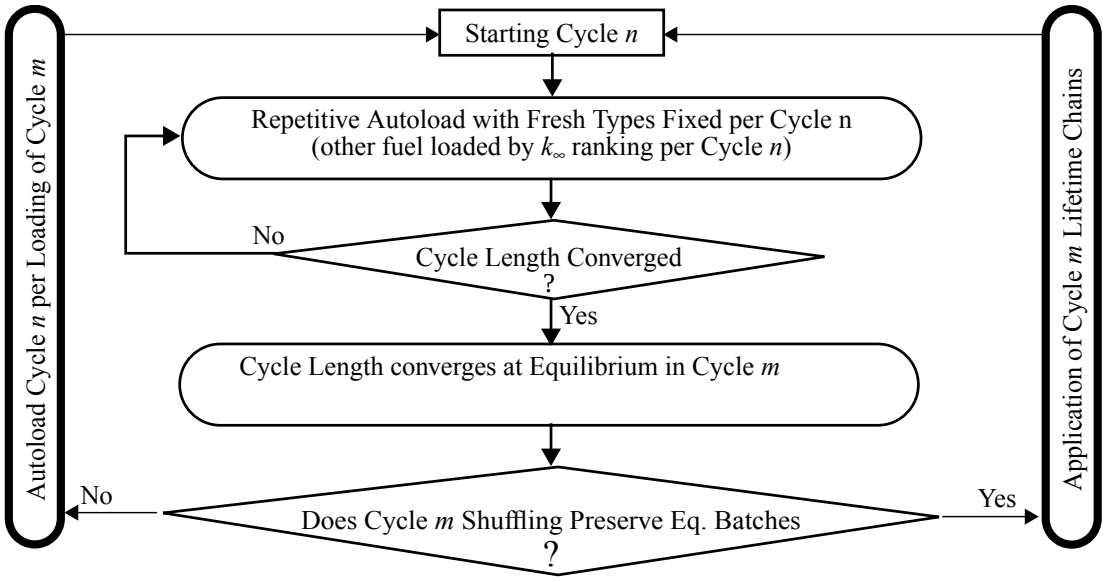

Consider an equilibrium core at Cycle *m*

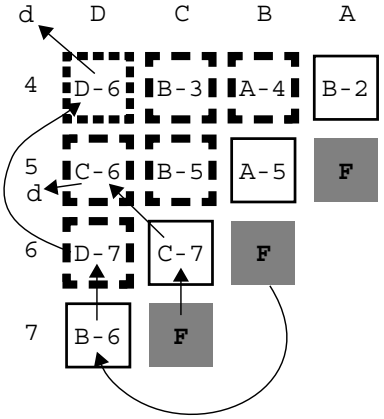

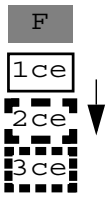

Lifetime chains for each fresh assembly:

Fresh B2→A4→B4→discharge

Fresh A5→B5→C5→discharge

Fresh B6→D7→D6→D4→discharge

Fresh C7→C6→D5→discharge

Fresh A3→B3→C4→discharge

Interactive shuffle of a depleted assembly into B-6 to reduce the fresh loading breaks a lifetime chain

This shuffle in Cycle *m* resulted in a non-equilibrium state of 8 Fresh, 12 Once, 12 Twice, 9 Thrice

The lifetime chain logic of the enhanced equilibrium search capability will alert the user to such a condition, and automatically revert to the autoloading process to arrive at the equilibrium associated with the altered inventory.

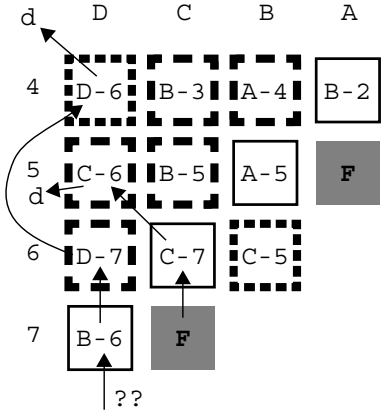

Fresh ??→C7→D6→D4→discharge

Fresh D7→C6→D5→B6→discharge

Fresh A4→B3→C4→B2→discharge

Fresh ??→A3→B4→discharge

Fig. 2: Design at Equilibrium via Automated Redepletion

The enhanced system is based on the following definition of equilibrium:

- fixed fresh fuel placement (i.e., same designs loaded into the same positions)
- consistent placement of all reloaded fuel, per the lifetime chain[8] from a fresh location, to a once-burned location, etc., through discharge
- converged cycle length

XIMAGE builds the lifetime chains of fuel from the actual fuel histories. If chains cannot be established for the initial scoping and transition cycles due to changes in batch size or the use of reinserted or cross-unit fuel, then the autoloader can be used to establish the equilibrium associated with the depleted k_∞ distribution of the initial core, per Figure 2. A rule set to fix fresh types is created by the XIMAGE equilibrium search process. Other rules (such as face peripheral history) can be applied during the equilibrium search process as well.

Figure 3 illustrates convergence to equilibrium from a transitional design. The model was the 3-loop PWR core with 157 assemblies described in detail in Reference 10. 72 assemblies were loaded in a "ring-of-fire" configuration for a cycle 4 length of 16.20 GWD/MT. Autoloading was applied to find the equilibrium since the increase in the number of fresh loaded made definition of lifetime chains impossible in cycle 4. As is typical, Figure 3 indicates large oscillation of cycle length for the first two search cycles, where the fuel inventory is not yet at equilibrium. The search then converges quickly to a cycle length of 15.62 GWD/MT. Note that the discharge burnup converges to 34.07 GWD/MT. This satisfies the classic[9] equilibrium relationship between cycle length and discharge burnup: discharge burnup = cycle burnup * (total assemblies / fresh assemblies).

Once an equilibrium is established, shuffling can be performed at the endpoint of the equilibrium process. Lifetime chains are preserved, as discussed by the example of Figure 2. The effect of the endpoint shuffles on the equilibrium can be evaluated by automatic redepletion from the initial cycle to equilibrium, per Figure 2. This process preserves rotation as well as placement, in the case of a PWR.

The ability to design at equilibrium without regard to the starting pattern is illustrated in Figure 4. The 3-loop core was loaded with the same fresh fuel, but in a poor configuration with short cycle length of 14.88 GWD/MT and highly infeasible $F_{\Delta H}$ of 2.050. But when the lifetime chains associated with the equilibrium of Figure 3 were

applied in an equilibrium search which began in cycle 5, then the same equilibrium with cycle length of 15.62 GWD/MT was achievement. The autoloaded equilibrium associated with the poor pattern is also shown, with endpoint of 15.28 GWD/MT.

Figure 4 demonstrates that the equilibrium point is insensitive to transitional cycles. The XIMAGE capability for interactive design at the equilibrium endpoint is a powerful tool for scoping studies considering new fuel designs or strategies.

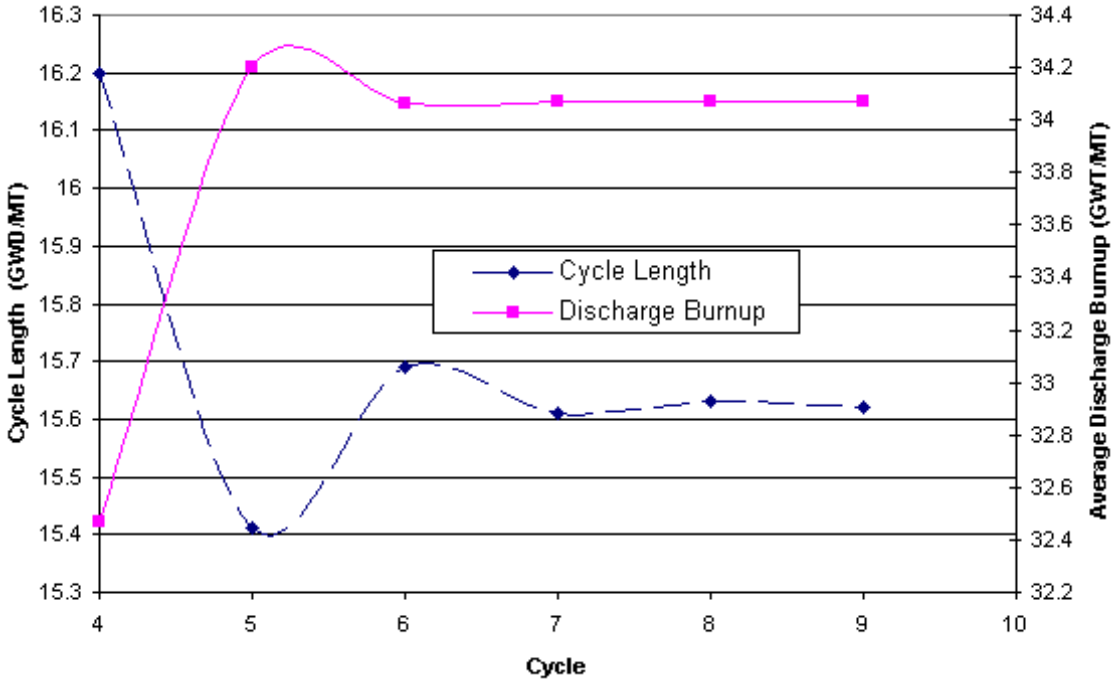

Fig. 3: Application of Autoloader Search for Equilibrium

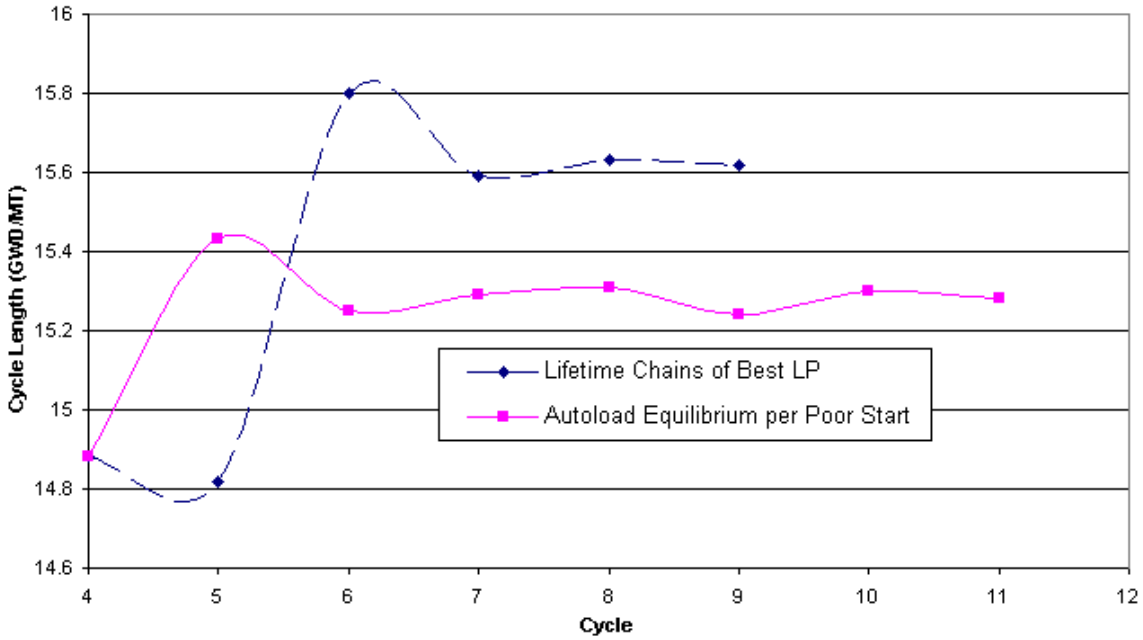

Fig. 4: Lifetime Chain Equilibrium Invariant to Starting Point

3. PWR SINGLE CYCLE OPTIMIZATION WITH SIMAN

The SIMAN PWR[10,11] optimization module automates design in three levels of search scope:

- an implementation of adaptive **simulated annealing**, a liberated search algorithm, including support for optional user-configurable heuristics to limit the design space of the search;
- a random **direct search** which uses the same candidate generator as the annealing algorithm, but only accepts candidates which offer direct improvement; and
- an **autosequence** to evaluate a collection of candidates, sorting the patterns per the configurable objective and constraint definitions used by the search options.

The SIMAN PWR module uses SIMULATE-3 directly, so results are both accurate and consistent with manual design. A broad range of 2D and 3D objective and constraint terms is available during optimization.

SIMAN PWR has also been enhanced to perform equilibrium searches in order to treat equilibrium cycle length as an objective or constraint. This is not yet practical during annealing or direct search optimizations. But, an autosequence run with equilibrium search allows results of the optimizations to be automatically run through equilibrium energy analyses and then sorted according to equilibrium energy as well as single cycle constraints (cycle length, F_Q, MTC, etc.).

4. EFFECT OF SINGLE CYCLE OPTIMIZATION ON EQUILIBRIUM PERFORMANCE

One of the classic arguments against the loading of novel patterns generated by optimization tools has been that improvements in one cycle will just be "paid for" in subsequent cycles. Stevens[10,12] and Kropaczek[13] independently used successive cycle optimizations to examine the validity of this concern. Yamamoto[8] then compared equilibrium optimizations and successive cycle optimizations explicitly. All three studies showed that single cycle optimizations did not inherently make successive cycle design too difficult (or suboptimal). Many single cycle optimization improvements reduce leakage and flatten power in sustainable ways.

Equilibrium analysis is useful in addressing this concern, since the final state of the equilibrium is independent of the transition cycles. Successive cycle optimizations suffered if transition cycle optimizations were truncated too quickly.

Figure 5 illustrates one case of an autoloaded pattern and an optimized pattern. Both patterns satisfy difficult constraints on $F_{\Delta H}$, F_Q, and MTCs for two year cycles. Shuffling was quite constrained for the two-year cycle design since limits on exposure under control rods essentially require fresh fuel under rods. 92 fresh assemblies were loaded into the core of 217 assemblies. Only four erbium loadings were considered for the fresh fuel. Nonetheless, the SIMAN PWR annealing result produced an additional 6.1 EFPD of HFP cycle length, to 631.6 EFPD, while still satisfying all constraints. Both patterns were depleted to equilibrium, as shown. The endpoint associated with the SIMAN PWR result maintained a slight advantage in cycle energy of 1.9 EFPD. Discharge burnups of the two equilibria were essentially the same.

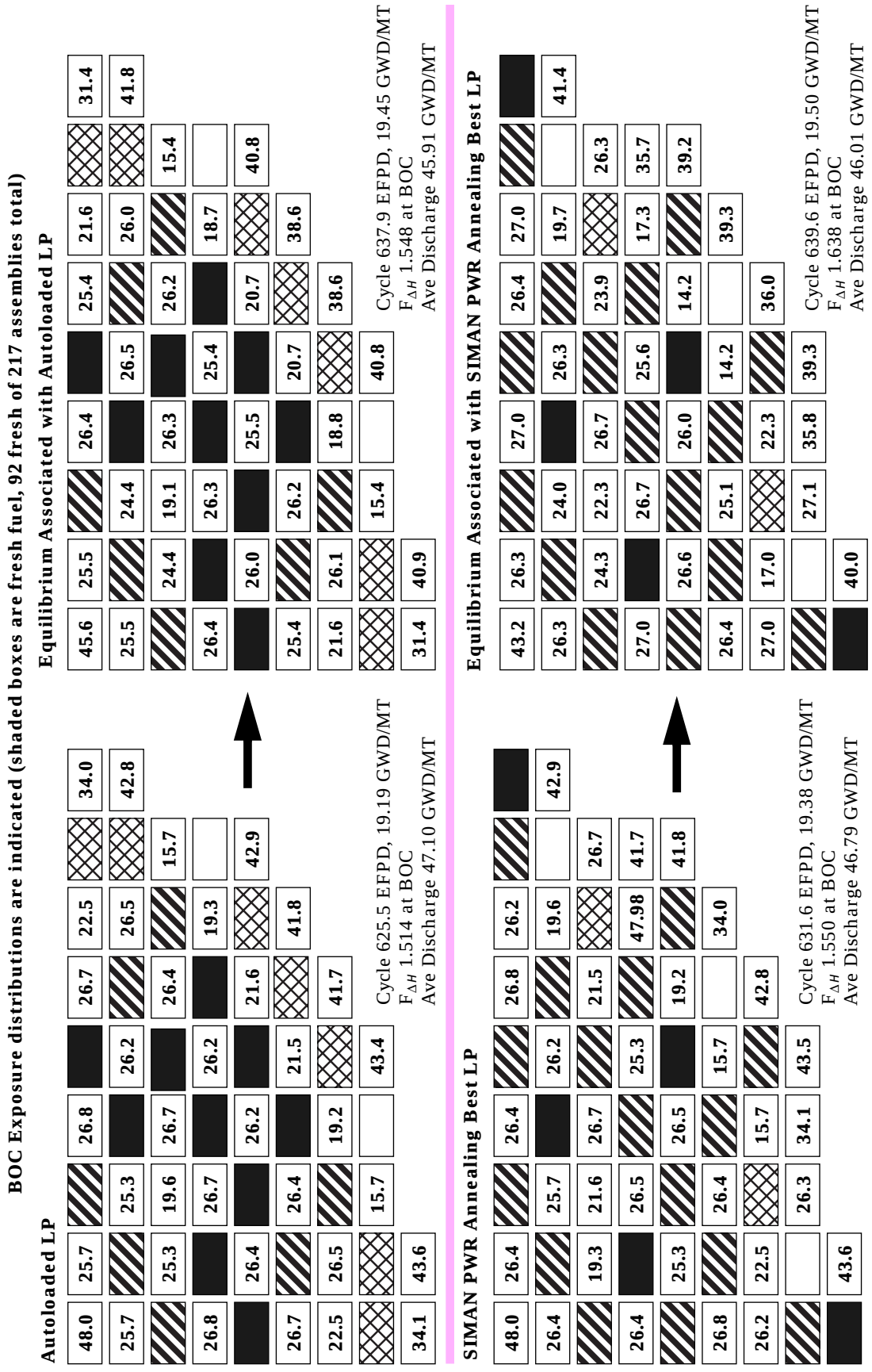

Fig. 5: Comparison of Autoloaded and Optimized LP Equilibria for a Two Year Cycle

Table 2 indicates how equilibria can evolve for more radical optimizations of the 3-loop PWR, per Figures 3 and 4. As was illustrated in Figure 4, the optimized pattern with cycle 4 length of 16.20 GWD/MTU maintained a large advantage over the poor starting guess. Table 2 also indicates the equilibrium search associated with an optimization to higher margin, with trade-off in cycle 4 length of 15.88 GWD/MTU. The higher margin pattern burns to an equilibrium of quality very similar to the best lp. The overall fuel utilization could be slightly better for the higher margin pattern, since the flatter power profile results in more even burnup of the fuel assemblies (a small advantage for spent fuel racking). But again, the aggressively optimized pattern (which began with an advantage of 8.7 EFPD in cycle 4 length) does not suffer at equilibrium (where an advantage of 1.1 EFPD still exists). The fact that less of the improvement is maintained would indicate that the optimization of the transition cycle did exploit the particular depleted fuel exposures available in the transition.

5. CONCLUSIONS

XIMAGE/SIMAN has been successfully extended to search for consistent equilibrium designs of both BWR and PWR reactors in order to judge the long term effects of single cycle optimization. Applications indicate that the common assumption that improvements in single cycle performance through optimization cannot be sustainable is often incorrect. Though some aggressive optimizations will surely lead to unsustainable results, the current tool allows the decision to accept or reject novel designs to be based on sound and consistent analysis rather than conjecture.

Furthermore, the related enhancements to XIMAGE/SIMAN simplify the explicit design of equilibrium cycles, which simplifies consistent comparison of different candidate fuel designs or loading strategies (both fuel and reactivity control).

ACKNOWLEDGEMENTS

The authors express their appreciation to Mr. Nobuyuki Nakagawa and Mr. Atsushi Shimoura of Nuclear Engineering, Ltd., Osaka, for their help defining and testing the lifetime chain shuffling method of equilibrium design.

Table 2: Comparison of Equilibrium Searches for 3-Loop Patterns

	Cycle	Cycle Length		Ave Discharge Burnup GWD/MT	Peak/Ave Discharge Burnup
		GWD/MT	EFPD		
SIMAN Starting LP Cycle 4 $F_{\Delta H}$ 2.050	4	14.88	404.1	32.67	1.242
	5	15.43	419.1	33.28	1.256
	6	15.25	414.3	33.36	1.287
	7	15.29	415.3	33.33	1.300
	8	15.31	415.9	33.36	1.292
	9	15.24	414.0	33.31	1.296
	10	15.30	415.5	33.32	1.293
	11	15.28	415.1	33.33	1.296
SIMAN Best LP Cycle 4 $F_{\Delta H}$ 1.440	4	16.20	440.1	32.47	1.254
	5	15.41	418.6	34.20	1.318
	6	15.69	426.1	34.06	1.315
	7	15.61	423.9	34.07	1.301
	8	15.63	424.5	34.07	1.306
	9	15.62	424.3	34.07	1.305
SIMAN High Margin Cycle 4 $F_{\Delta H}$ 1.408	4	15.88	431.4	32.63	1.112
	5	15.48	420.3	34.00	1.241
	6	15.60	423.8	34.00	1.191
	7	15.58	423.2	33.98	1.175
	8	15.58	423.2	33.98	1.180

REFERENCES

1. D. J. Kropaczek and P. J. Turinsky, "In-Core Nuclear Fuel Management Optimization for Pressurized Water Reactors Utilizing Simulated Annealing," *Nucl. Technol.*, **95**, 9 (1991).
2. J. Rhodes et al., "X-IMAGE: A SIMULATE-3 Based Graphical User Interface for Interactive Core Design," *Proc. Topl. Mtg. Mathematical Methods and Supercomputing in Nuclear Applications*, Karlsruhe, Germany, April 19-23, 1993, **2**, 642 (1993).
3. B. J. Johansen, "ALPS: An Advanced Interactive Fuel Management Package," *Proc. Topl. Mtg. Adv. Reactor Phys.*, Knoxville, TN, April 11-15, 1994, **III**, 324 (1994).
4. J. G. Stevens and K. R. Rempe, "Recent Enhancements in the X-IMAGE/SIMAN Core Design Environment," *Proc. Topl. Mtg. Advances in Nuclear Fuel Management II*, Myrtle Beach, SC, March 23-26, 1997, **1**, 8-19 (1997).
5. J. T. Cronin, K. S. Smith, and D. M. Ver Planck, "SIMULATE-3 Methodology," SOA-95/18, Studsvik of America (1995).
6. M. Edenius et al., "CASMO-4: A Fuel Assembly Burnup Program, User's Manual," STUDSVIK/SOA-95/1, Studsvik of America (1995).
7. S. Palmtag, "PWR Steaming Rate Model in CMS" SSP-00/429 Rev. 1, Studsvik Scandpower (2002).
8. A. Yamamoto and K. Kanda, "Comparison between Equilibrium Cycle and Successive Multicycle Optimization Methods for In-Core Fuel Management of Pressurized Water Reactors," *J. Nucl. Sci. Technol.*, **34**, 882 (1997).
9. M. J. Driscoll, T. J. Downar, E. E. Pilat, *The Linear Reactivity Model for Nuclear Fuel Management*, Am. Nucl. Soc., La Grange Park, Illinois(1990).
10. J. G. Stevens et al., "Optimization of Pressurized Water Reactor Shuffling by Simulated Annealing with Heuristics," *Nucl. Sci. Eng.*, **121**, 67 (1995).
11. S. G. Zimmerman and J. A. Umbarger, "Design of Aggressive Loading Patterns with X-IMAGE/SIMAN for Palo Verde Nuclear Generating Station," *Proc. Topl. Mtg. Advances in Nuclear Fuel Management II*, Myrtle Beach, SC, March 23-26, 1997, **2**, 16-17 (1997).
12. J. G. Stevens et al., "Simplified Automated Loading Pattern Generation for Multicycle Analysis," *Trans. Am. Nucl. Soc.*, **69**, 420 (1993).

13. D. J. Kropaczek, J. McElroy and P. J. Turinsky, "Validity of Single-Cycle Objective Functions for Multicycle Reload Design Optimization," *Trans. Am. Nucl. Soc.*, **69**, 419 (1993).